MIT Libraries | DSpace@MIT

MIT Open Access Articles

Understanding why the thinnest SiNx interface in transition-metal nitrides is stronger than the ideal bulk crystal

The MIT Faculty has made this article openly available. ***Please share*** how this access benefits you. Your story matters.

Citation: Zhang, R.F., A.S. Argon, and S. Veprek. "Understanding why the thinnest SiNx interface in transition-metal nitrides is stronger than the ideal bulk crystal." Physical Review B 81.24 (2010): 245418. © 2010 by American Physical Society

As Published: http://dx.doi.org/10.1103/PhysRevB.81.245418

Publisher: American Physical Society

Persistent URL: http://hdl.handle.net/1721.1/60890

Version: Final published version: final published article, as it appeared in a journal, conference proceedings, or other formally published context

Terms of Use: Article is made available in accordance with the publisher's policy and may be subject to US copyright law. Please refer to the publisher's site for terms of use.

Massachusetts Institute of Technology

Understanding why the thinnest SiN_x interface in transition-metal nitrides is stronger than the ideal bulk crystal

R. F. Zhang,[1] A. S. Argon,[2] and S. Veprek[1,*]
[1]*Department of Chemistry, Technical University Munich, Lichtenbergstr. 4, D-85747 Garching, Germany*
[2]*Department of Mechanical Engineering, Massachusetts Institute of Technology, 77 Massachusetts Avenue, Cambridge, Massachusetts 02139, USA*
(Received 13 November 2009; revised manuscript received 15 May 2010; published 15 June 2010)

One-monolayer-thick SiN_x interfacial layer in superhard nanocomposites, consisting of 3–4 nm size TiN nanocrystals joined by that layer, is stronger than a bulk SiN_x crystal due to valence charge transfer from the metallic TiN, thus providing the nanocomposites with significant hardness enhancement. However, this enhancement is lost when the thickness of the interfacial SiN increases to ≥2 monolayers and the hardness decreases. We show that the softening of the nanocomposites with thicker SiN_x interface is caused by the weakening of the TiN bonds close to that interface, that increases with increasing of the SiN_x thickness. Other possible mechanisms of the softening are briefly discussed and ruled out. This finding may open up possible way of preparing new, even stronger superhard nanocomposites.

DOI: 10.1103/PhysRevB.81.245418 PACS number(s): 68.35.Gy, 62.20.Qp, 62.25.−g

I. INTRODUCTION

Grain boundaries and interfaces in most solids are characterized by increased (destabilizing) energy of formation, and thus represent the weak links as compared to bulk crystals.[1,2] Only coherent interfaces with small lattice mismatch, such as twin boundaries, can reach strength approaching that of the bulk matrix but never exceed it. For example, in ductile metals where ductile fracture initiates by decohesion of high-quality particles, such as Fe_3C and TiC in iron, experiments indicated that while interface decohesion strengths could be as high as 0.9% of the Young's modulus of Fe, they never reach the cavitation strengths of the latter.[3,4] The only case known to us, where an interface is stronger than the bulk, is when about one-monolayer (1-ML) thick SiN_x is sandwiched between slabs (in heterostructures) or nanocrystals (in nanocomposites) of a hard transition-metal nitride, such as TiN, ZrN, WN, VN, and others. First-principles theoretical calculations have shown that one 1-ML-thick Si_3N_4-like,[5,6] or fcc(NaCl)-like 1 ML SiN layer, heteroepitaxially stabilized between TiN slabs,[7] has significantly higher decohesion[5] as well as shear[7] strength than the corresponding bulk crystal. Many experiments have shown that, in the nanocrystalline (nc)-*Tm*N/x-ray amorphous (a)-Si_3N_4 [*Tm*=Ti, W, V, $(Al_{1-x}Ti_x)N$, and other transition metals] and in nc-TiN/a-BN nanocomposites,[8] the maximum hardness is obtained when the thickness of this layer is about 1 ML, and it strongly decreases with a further increase in that thickness.[9,10] Also experiments on the deposition of heteroepitaxial TiN/SiN (Refs. 11–15) and ZrN/SiN heterostructures[16] revealed that maximum hardness is achieved when the SiN thickness is about 1–2 ML. Thus, the enhanced strength of the 1 ML SiN_x interface should be fairly general.

Pseudomorphically stabilized fcc-SiN-like interfacial layers are present in TiN/1 ML SiN/TiN heterostructures, which were deposited by dual magnetron sputtering. This layer is formed during the deposition of SiN on several nanometer thick fcc-TiN template slab, and it collapses when its thickness increases to about ≥3 ML.[11–15] Although the bulk fcc-SiN is inherently unstable against small-amplitude phonon vibrations (within the harmonic approximation) at zero pressure in its highly symmetric fcc configuration,[17] the 1 ML (111) and (110) interfaces sandwiched between TiN slabs are stable against finite distortion of ≤3%.[18,19] Only the 1 ML (001) interface is inherently unstable (see Table I in Ref. 18), in agreement with its dynamic instability from phonon calculation,[17] but it can be stabilized by finite distortion of about 12% in the [110] direction that lowers its symmetry and decreases its energy to a local minimum, which is stable against finite distortions (see Figs. 1 and 2 in Ref. 18 and the discussion below). Of course, the stability of the (111), (110), and of the distorted (001) interfaces against finite displacements does not assure their phonon stability with respect to other phonon vectors within the whole Brillouin zone. Such calculations would require a huge computational effort that is beyond the scope of our paper. Moreover, as we already mentioned, we focus here on the SiN interfacial layer which has been identified by Hao *et al.*[5,6] to be the weakest one of all possible SiN_x interfaces including the thermodynamically stable Si_3N_4-like ones. Because, as it will be shown, the weakening of the TiN/SiN/TiN system with SiN thickness of ≥2 ML is due to progressively increasing weakening of the neighbor Ti-N bonds, the conclusions of our present paper should apply also to the stronger and thermodynamically stable Si_3N_4-like interfaces.

The maximum hardness of the heterostructures is reached when the SiN interface is about 1 ML thick, and it decreases when the thickness is ≥2 ML,[11] in an analogy with the nanocomposites. However, there are some important differences between the heterostructures and the nanocomposites with randomly oriented nanocrystals. [The random orientation of the nanocrystals has been shown experimentally for a variety of nc-*Tm*N/a-Si_3N_4 and nc-TiN/a-BN nanocomposites, in particularly for the nc-TiN/a-Si_3N_4 by x-ray diffraction (XRD) (Refs. 10 and 20) and high-resolution transmission electron microscopy.[21]] Two most important differences are: (a) in order to meet the compatibility condition, all slip

 ©2010 The American Physical Society

systems have to shear upon plastic deformation in the nanocomposites with randomly oriented nanocrystals, whereas a single crystal will deform along the easiest slip system. This may explain why much lower hardness maximum of about 35 GPa has been achieved in the heterostructures as compared with the superhard nanocomposites.[7,9,10] (b) The heterostructures have only one crystallographic type of the SiN_x interface, depending on their orientation. In contrast, many different interfaces have to coexist in the nanocomposites, including strong as well as some weaker ones, but all have to shear upon plastic deformation.[7]

High-pressure XRD studies have shown that the TiN nanocrystals deform only elastically whereas the plastic deformation occurs by shear within or in the vicinity of the grain boundaries.[22] For these reasons we limit our present studies to the SiN interface, which is among the weakest ones and thermodynamically unstable under a sufficiently high nitrogen activity.[23] We concentrate on the fcc-TiN/SiN/TiN interface because the Ti-Si-N system has been studied in much more detail than the other *Tm*-Si-N or Ti-B-N ones.

The enhancement of the strength of the SiN_x interface is due to strengthening of the covalent Si-N bond across the interface by valence charge transfer from the TiN that has a high density of delocalized electrons at the Fermi level[5–7] and, therefore, is of metallic nature. However, the exact mechanism of the decrease in the hardness, when the thickness of that interface increases above 1 ML, has not yet been clarified. Several possible reasons for this softening were suggested but not unambiguously confirmed. We summarize them briefly.

(1) Because equilibrium Si-N bonds (0.1764 nm) are much shorter than Ti-N ones (0.2129 nm),[24,25] there is a tensile misfit stress within this interface which can be observed by XRD as lattice dilatation of the TiN nanocrystals.[26] With increasing thickness of a heteroepitaxial layer having a nonzero misfit to the substrate, the elastic strain energy proportionally increases up to a certain critical thickness, where it is energetically favorable to relax that energy by forming misfit dislocations.[27,28] Based on the well-known equilibrium relationship between the critical thickness and misfit, it has been suggested that for the nc-TiN/a-Si_3N_4 nanocomposites, this mechanism may limit the thickness of the SiN_x interfacial layer to about 1 ML.[28] However, one may raise two objections: (a) the formation of misfit dislocations in nanoscale systems is rarely possible. (b) The equilibrium theory, on which this correlation is based,[27] does not apply because the nanocomposites are deposited at relatively low temperature of 550–600 °C, where a much thicker heteroepitaxial layer may be kinetically stabilized due to the high activation energy needed for the formation of the dislocations, as known, e.g., from the $Si_{1-x}Ge_x$ system.[27]

(2) In the case of the fcc-TiN/SiN/TiN heterostructures (but not generally for the nc-TiN/a-Si_3N_4 nanocomposites which have higher thermal stability[9,10] than the heterostructures[29]), it may alternatively be argued that the thicker fcc-SiN layer collapses due to an inherent dynamic instability of that phase, as suggested in Ref. 17. In our earlier paper,[18] we have studied the static stability (which may be related to the limit of long-wave phonons) of 1-ML-thick (111), (110), and (001) interfaces by imposing a distortion of

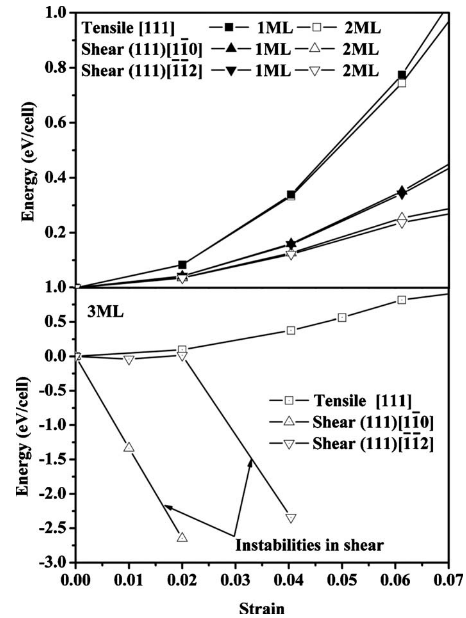

FIG. 1. The change in the total energy with strain of the modeled (111) TiN/SiN/TiN interfaces with one, two, and three monolayers of SiN, which reflect the instability of 3 ML under small shear-strain deformation.

3% in different crystallographic directions and calculating the change in the total energy by means of *ab initio* density-functional theory (DFT). As shown in Table I of that paper, the (111) and the (110) interfaces are stable but the (001) is unstable against such distortion. The instability of (001) interface is in agreement with the results from dynamical stability.[17] Interestingly, as seen in Figs. 1 and 2 of that paper, the (001) interface can reach a stabilized state upon a distortion of the Si atoms in the [110] direction by about 12% where a minimum of the total energy occurs. We refer to our recent paper[18] for further details.

The stabilization of a system by lowering its symmetry is well known in many crystalline solids[30,31] and complex molecules.[32] Besides, there are examples where structures, which are dynamically unstable in bulk, can be stabilized as

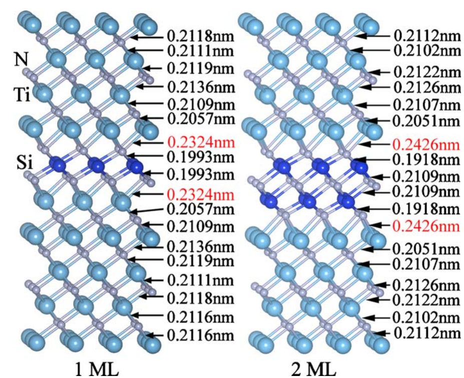

FIG. 2. (Color online) The atomic structures and the variations in bond lengths of the modeled (111) TiN/SiN/TiN interfaces, which reflect the oscillations of valence charge density shown in Fig. 2 with (left) 1 ML SiN (Ref. 19) and (right) 2 ML SiN in equilibrium after full relaxation of the cell.

thin films by heteroepitaxial growth or even by the deposition on glass substrate. For example, fcc-Ni is the stable phase of nickel, but the dynamically unstable bcc-Ni, which does not exist in the nature as bulk, has been stabilized by heteroepitaxial growth on GaAs (001).[33] Furthermore, the dynamically unstable bcc-Ni has been obtained in nanocrystalline form upon severe plastic deformation by room-temperature rolling of the stable fcc-Ni.[34] Also fcc tungsten displays dynamic phonon instability as shown by *ab initio* DFT calculations,[35] but it has been stabilized as thin films by deposition on a variety of substrates (pyrex glass, mica, NaCl) even at deposition temperature up to 400 °C. It transformed to the stable phases only upon subsequent heating to 700 °C.[36–38] These examples show that a phase, which is dynamically unstable in bulk, can be significantly stabilized as nanocrystalline material.

As it has been shown by the Linköping[11–14] and other[15] groups, the fcc-TiN/SiN/TiN heterostructures reached maximum hardness when the thickness of the fcc-SiN interfacial layer was about 1 ML, but it decreased and the fcc-SiN collapsed when its thickness exceeded several monolayers. The hardness of the nc-*Tm*N/a-Si_3N_4 nanocomposites reached a maximum for about 1-ML-thick Si_3N_4-like interface, but it strongly decreased when the thickness increased to 2 ML. Therefore, the question arises if this decrease is due to incipient electronic instability of the ≥ 2 ML SiN interface. Of course, a test of a dynamical stability would be helpful for the understanding of the stability of the studied interface structures. However, such a test will be quite challenging and time consuming and may not be easily accomplished with reliable precision in a reasonable time. In view of this, we would like to emphasize that the present studies are limited to only the static stability where the interface systems studied are stable provided no phonons with imaginary frequency occur within the Brillouin zone at momentum larger than zero.

(3) The third possibility, which might explain the observed softening, involves electronic weakening of the TiN/1 ML SiN/TiN system with increasing thickness of the SiN interface, due either to a decreasing enhancement of the valence charge transfer to the SiN interface or to an increasing weakening of the neighboring TiN as a result of the oscillations of Ti-N bond distances and their strength, as discussed for 1 ML in Refs. 18 and 19. In this paper we shall show that the latter mechanism gives the correct explanation: The 2 ML SiN interface remains strong, but the neighbor TiN crystals are progressively weakened by these oscillations with increasing thickness of that interface to 2 ML. This finding is based on the earlier experimental results mentioned above, it should apply generally to many other *Tm*N/SiN_x systems that form superhard nanocomposites.[9,10]

II. CALCULATION METHOD

Our *ab initio* DFT calculations were done using the "Vienna *ab initio* simulation package" code[39] with the projector augmented wave method employed to describe the electron-ion interaction[40] and the generalized-gradient approximation for the exchange-correlation term together with the Vosko-Wilk-Nusair interpolation. The integration in the Brillouin zone has been done on special *k* points of $5 \times 5 \times 3$ grids for the interface systems, determined according to the Monkhorst-Pack scheme, energy cutoff of 600 eV, and the tetrahedron method with Blöchl corrections for the charge-density calculation, and Gaussian smearing for the stress calculations. The method of the calculation of the stress-strain response and electronic structure has been described and carefully verified in our earlier papers to which we refer the readers for further details.[24,25,41]

III. RESULTS

A. Equilibrium interface structure

The crystallographic Miller's indices indicated for the (111) interface modeled here are, in the following text, marked with respect to the cubic unit cell of fcc(NaCl)-TiN. The TiN layered structure is obtained from fcc(NaCl)-type unit cell with $\langle 1\bar{1}0 \rangle$, $\langle \bar{1}\bar{1}2 \rangle$, and $\langle 111 \rangle$ as *x*, *y*, and *z* Cartesian coordinate axes to model the (111) layers. The coherent TiN/SiN/TiN (111)-type interface models with one, two, and three monolayers pseudomorphic SiN interfacial layer are constructed by replacing one, two, and three Ti layers in the middle by Si atoms. Afterward, the modeled TiN/SiN/TiN interfaces are fully relaxed to get an equilibrium stable geometry and to compare the bond length and electronic structure of the interfaces. We note that the relaxed 1 ML and 2 ML (111) interfaces are energetically stable against small displacements[18,19] and homogeneous distortion in tension and shear as shown in Fig. 1 (see remark in Ref. 42), because the total energy increases with increasing strain due to the increasing elastic energy. However, the total energy strongly decreases with increasing strain for the 3 ML interface (Fig. 1), thus showing its instability upon applied small strain. We do not discuss this case further here because the behavior of the 2 ML SiN interface and of the neighbor TiN is sufficient to explain the observed softening of the nanocomposites and heterostructures for interface thicker than 1 ML, which is the focus of the present paper. The relaxed atomic structures for 1 ML and 2 ML SiN interfaces are shown in Fig. 2 to illustrate the difference of the oscillations of bond lengths for the different thicknesses of the SiN layers.

The oscillations of bond lengths shown in Fig. 2, damped with increasing distance from the SiN interface, reflect the oscillations of valence charge-density difference shown in Fig. 3 which is the result of valence charge transfer from the metallic TiN to the SiN due to a higher electronegativity of Si as compared with Ti. One notices in Fig. 2 that the Si-N bond lengths of 0.1993 nm and 0.1918 nm for one and two monolayers, respectively, (in the later case we refer to the bonds on the border between the 2 ML SiN interface and the TiN), are significantly shorter than those in bulk fcc-SiN crystal (0.2131 nm) and only slightly longer than that in stoichiometric, stable bulk hcp(β)-Si_3N_4 (0.1764 nm).[24] These bond lengths are shorter for the 2 ML interface as compared to 1 ML, thus suggesting a further stabilization of the 2 ML SiN interface. The Si-N bonds lengths in the middle of the 2 ML SiN interface of 0.2109 are longer, albeit

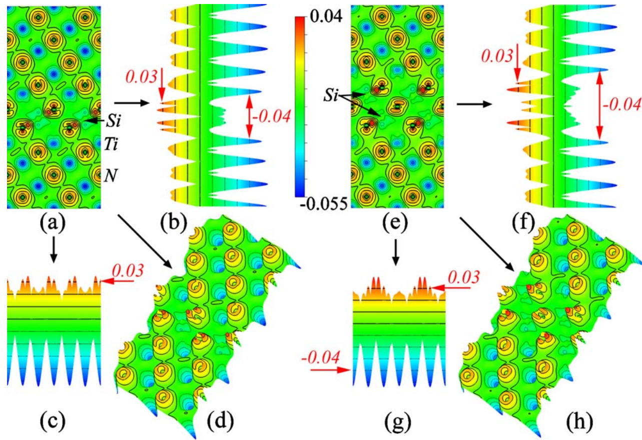

FIG. 3. (Color online) Valence charge-density difference of 1 ML [left, (a)–(d)] and 2 ML [right, (e)–(h)] SiN interface with TiN slabs above and below. (a) is the top view, (b) and (c) the side views as indicated, and (d) is the perspective view of the sandwich with 1 ML SiN interface. (e)–(h) are the corresponding views for the sandwich with 2 ML SiN interface. The color scale runs from −0.055 at bottom blue to 0.04 e/bohr^3 at top red. The small (red) italic numbers indicate the values of the VCDD.

shorter than those in bulk fcc-SiN thus indicating some decrease in the strengthening therein. However, the Ti-N bonds in the layer next to the SiN interface have the largest length of 0.2324 nm and 0.2426 nm for one and two monolayers, respectively (Fig. 2), significantly larger than that of bulk fcc-TiN of 0.2129 nm. This bond is about 5% longer for 2 ML than for 1 ML interface, which documents the enhanced weakening of this bond in the case of the thicker SiN interface as observed in experiments.[9,10]

Figure 3 shows the calculated valence-charge-density difference (VCDD; defined as the difference between the calculated valence charge density of the crystal minus those of neutral atoms at the given lattice sites) for one- and two-monolayers-thick SiN (111) interfaces. One notices that the SiN interface is stabilized by negative charge transfer to nitrogen in both cases, and the VCDD is larger on Si than on Ti atoms. Interestingly, the VCDD on N atoms bonded to neighbor Ti ones is enhanced for 2 ML as compared to 1 ML interface, and the VCDD on N atoms in the middle of the 2 ML interface (cf. Figs. 2 and 3) is lower than that on the N atoms in 1 ML one. These atoms are bonded to Si only (cf. Fig. 2). Thus, one can clearly see that although the SiN is becoming less stable for 2 ML, the pseudomorphic stabilization by the negative valence charge transfer to the N atoms within the 2 ML SiN interface next to TiN overcompensates the inherent electronic instability of bulk SiN also for the 2 ML interface.

B. Stress-strain response in tension and shear

In the following part, we shall study the behavior of the system upon decohesion (relevant for crack growth and brittle fracture) and shear (relevant for plastic deformation; see remark Ref. 42). Figure 4 compares the stress-strain curves in tensile [perpendicular to the (111) interface] and in

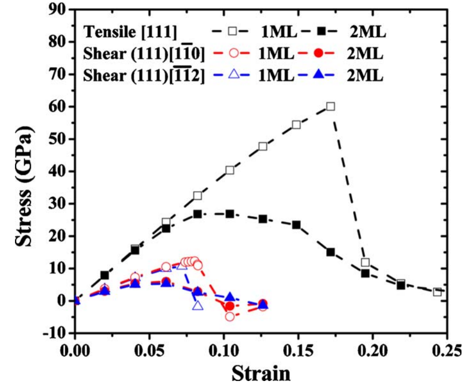

FIG. 4. (Color online) Calculated stress-strain curves of (111) TiN/1 ML-SiN/TiN and TiN/2 ML-SiN/TiN interfaces for the tensile and shear modes of deformation as indicated.

shear loading (within that interface) for 1 ML and 2 ML SiN interfaces. As expected, the heterostructure with 2 ML SiN interface is significantly weaker in all cases, but still stronger than the bulk because the lowest shear strength in the case of the 2 ML interface of 5 GPa (Fig. 4) is still larger than that of bulk SiN of about 3 GPa.[7,24] Moreover, whereas all stress-strain curves of the 1 ML SiN interface show, upon the decohesion or shear instability, an abrupt decrease in the stress, their corresponding counterparts for 2 ML interface are relatively smooth. In the case of the 1 ML interface, the valence charge density remained topologically intact up to the highest stress corresponding to a normal strain of $\varepsilon=0.1717$ and the decohesion occurred only after the instability at strain $\varepsilon=0.1951$ (see Fig. 4).

In order to illustrate the different decohesion behavior of the 1 ML and 2 ML interfaces in more detail, we show in Fig. 5 the atomic structures with the low values of the isosurface of VCD (IVCD) of 0.015 e/bohr^3 for several relevant tensile decohesion states as indicated in that figure (see Fig. 4 for the relevant stress-strain curves). The very small value of the VCD of 0.015 e/bohr^3 represents the situation close to the borderline when the bonds break, i.e., the corresponding isosurfaces show where the decohesion occurs.

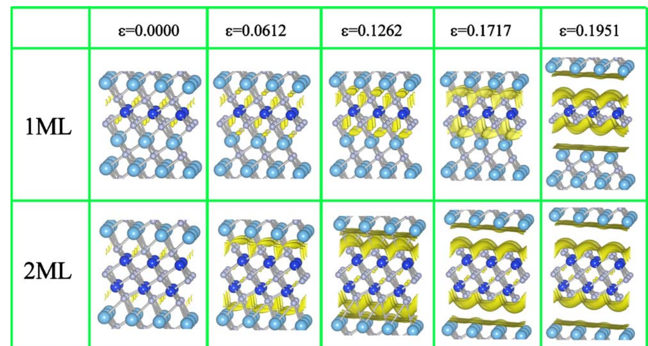

FIG. 5. (Color online) Isosurfaces of valence charge density corresponding to very small value of valence charge density of 0.015 e/bohr^3 during the given values of applied tensile strain to (111) TiN/2 ML SiN/TiN interface along the direction normal to that interface (cf. the corresponding stress-strain curves in Fig. 4).

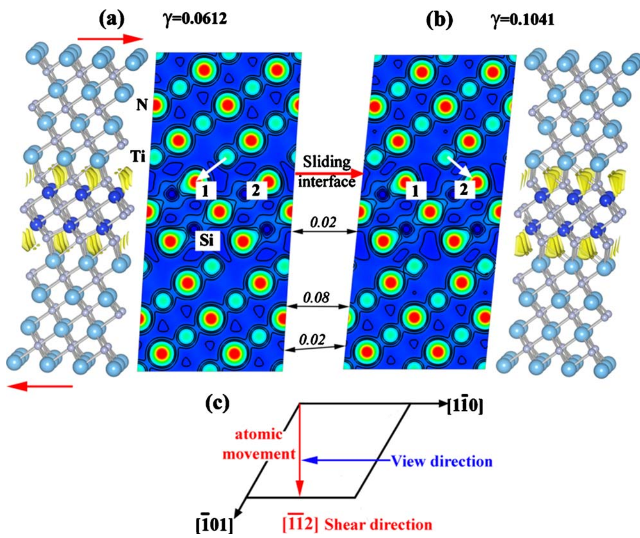

FIG. 6. (Color online) VCD and IVCD corresponding to a very small value of VCD of 0.015 e/bohr^3 of the (111) interface upon shear applied in the weak $[\bar{1}\bar{1}2]$ direction at strain of (a) $\gamma=0.0612$ and of (b) $\gamma=0.1041$. The white arrow shows the flip-over of the Ti-N bond from atom Ti(1) to Ti(2) due to the shear event. (c) The top view normal to the (111) interface showing the orientation of movement of the atoms and view direction. The VCD scales from 0 for dark blue to 0.5 e/bohr^3 for red color.

To spare space, we show only the part of the figures around the interfaces because no changes were seen within the remote TiN regions. There is not much difference in IVCD at equilibrium ($\varepsilon=0$) between the 1 ML and 2 ML interfaces. An onset of decohesion at strain $\varepsilon=0.0612$ is seen for 2 ML interface that is essentially completed at strain $\varepsilon=0.1262$ because there is no overlap between the IVCD of TiN and those of the 2 ML SiN interface. However, only small changes in IVCD are found for 1 ML interface at that strain. The onset of decohesion of the 1 ML interface is seen at strain of 0.1717 just before the instability (maximum tensile stress, see Fig. 4) with IVCD contours similar to those of 2 ML interface at a strain of $\varepsilon=0.0612$, whereas the TiN slab and 2 ML SiN interface are fully separated. After the instability, the decohesion of 1 ML SiN interface is completed thus underlining the discrete character of that decohesion, and the IVCD contours are similar for both interfaces. One notices that for both, 1-ML- and 2-ML-thick SiN interface the decohesion occurs on either side of the symmetrical interface. This is a consequence of the maintaining, during the calculation, the ideal structure of the system and perfect symmetry of the tensile load during the atomic relaxation. In a real experiment, the load will not be perfectly symmetric and any infinitesimal perturbation or even a flaw will select one side for separation, thus requiring lower energy.

Figure 6 shows the VCD distribution and IVCD of the (111) interface in shear applied in the soft $[\bar{1}\bar{1}2]$ direction at strain of $\gamma=0.0612$ and $\gamma=0.1041$ corresponding to the atomic arrangement just before [Fig. 6(a)] and after [Fig. 6(b)] the flip-over of the Ti-N bonds from atom N1 to N2. Clearly, the shear occurs between the Ti-N bonds weakened by the oscillations of the valence charge density (see Fig. 2) but not within the 2 ML SiN interface. In our recent paper[19] we considered the slightly stronger $(111)[1\bar{1}0]$ slip system and found that the movement of the atoms within the shearing plane occurs not in the $[1\bar{1}0]$ direction but in a zigzag manner in the energetically more favorable, complementary $[1\bar{1}2]$ and $[2\bar{1}\bar{1}]$ directions. In the present case of the easiest $(111)[\bar{1}\bar{1}2]$ slip system, the atomic movement is parallel to the applied shear stress. As in the case of the decohesion, the VCD and Si-N bond distances within the 2 ML interface remain essentially unchanged as compared with those in equilibrium at zero strain.

IV. SUMMARY

In conclusion, the results presented in this paper show that the 2-ML-thick (111) SiN interfacial layer remains strengthened by valence charge transfer, in analogy with the 1 ML of SiN and with the Si_3N_4 one. The observed decrease in the hardness of the nc-TiN/a-Si_3N_4 nanocomposites and fcc-TiN/SiN/TiN heterostructures for the SiN_x thickness larger than one monolayer is due to the increasing weakening of the Ti-N bonds attached to that interfacial layer, as result of the increase in the amplitude of oscillations of valence charge density next to that interface which is the result of a larger electronegativity of Si as compared with Ti. The other possible mechanisms, discussed in the introduction, can be ruled out. In spite of the weakening of TiN that is observed already for the 1 ML SiN interface, the overall effect results in substantial strengthening of the TiN/1 ML SiN_x/TiN systems with superhardness of the nanocomposites[7,9,10] because bulk TiN is stronger than Si_3N_4 and SiN.[5,6,18,19] This is a unique case where a covalently bonded SiN_x interfacial layer strengthens the system, because in all other cases known to us, interfaces and grain boundaries are weaker than their bulk counterparts. Similar conclusions are likely to apply also for the Si_3N_4-like interfaces studied by Hao *et al.*[5,6] and to other nc-*Tm*N/a-SiN_x systems which form superhard nanocomposites.[9,10] Thus, further and more detailed studies are demanding.

In our earlier paper we have shown that the significant enhancement of the hardness of these nanocomposites can be easily understood when considering also other interfaces that occur in these systems with randomly oriented TiN nanocrystals.[7] In a recent paper Veprek-Heijman *et al.*[43] provided an independent experimental verification of such a high hardness and also of the validity of the Tabor's relation used in Ref. 7. In the present paper we limited our study only to the threefold symmetrical (111) interface because the other ones, such as (100) and (110) are much more complicated.[18] Consequently, much larger computational effort would be needed without revealing any substantially new physics.

Unlike many materials that have been recently synthesized in attempts to prepare new superhard materials (e.g., Refs. 44 and 45), the superhard nanocomposites nc-*Tm*N/a-Si_3N_4 with hardness of ≤ 50 GPa, limited only by impurities and relatively low deposition temperature that can be presently achieved in the large-scale industrial coating equipment,[46] are in industrial use. Deposited as wear protec-

tion coatings on tools for machining (drilling, turning, milling, cutting), forming, stamping and the like at relatively low costs, comparable to conventional hard coatings, they perform much better. In many industrial applications, tools coated with the nanocomposites enable significantly faster machining, longer lifetime of the coated tools and overall increase in the productivity at relatively low costs (see the recent invited review in Ref. 47).

ACKNOWLEDGMENTS

This work has been supported by the German Research Foundation (DFG), and by the European Commission within the project NoE EXCELL, Contract No. 5157032. The research of A.S.A. at MIT was supported by the Department of Mechanical Engineering of MIT. We thank Maritza Veprek-Heijman for many valuable comments.

---

*Corresponding author. FAX: +49 89 28913626; stan.veprek@lrz.tum.de

[1] D. A. Porter and K. E. Easterling, *Phase Transformations in Metals and Alloys*, 2nd ed. (Nelson Thornes, Cheltenham, U.K., 2000).

[2] A. S. Argon, *Strengthening Mechanisms in Crystal Plasticity* (Oxford University Press, Oxford, 2008).

[3] A. S. Argon, J. Eng. Mater. Technol. **98**, 60 (1975).

[4] A. S. Argon and J. Im, Metall. Trans. **6A**, 839 (1975).

[5] S. Hao, B. Delley, S. Veprek, and C. Stampfl, Phys. Rev. Lett. **97**, 086102 (2006).

[6] S. Hao, B. Delley, and C. Stampfl, Phys. Rev. B **74**, 035402 (2006).

[7] S. Veprek, A. S. Argon, and R. F. Zhang, Philos. Mag. Lett. **87**, 955 (2007).

[8] Here nc stands for nanocrystalline, a-for x-ray amorphous, and the stoichiometry Si_3N_4 express the fact that the binding energy of the Si 2*p* line as measured by XPS agrees exactly with that in the stoichiometric silicon nitride, i.e., Si atoms are fourfold coordinated to nitrogen. Of course, in the nanocomposites with randomly oriented TiN nanocrystals, many different (*hkl*) interfaces have to coexists and the exact stoichiometry of the SiN_x interface may somewhat vary (see reviews in Refs. 9 and 10).

[9] S. Vepřek, J. Vac. Sci. Technol. A **17**, 2401 (1999).

[10] S. Veprek, M. G. J. Veprek-Heijman, P. Karvankova, and J. Prochazka, Thin Solid Films **476**, 1 (2005).

[11] H. Söderberg, M. Oden, J. M. Molina-Aldareguia, and L. Hultman, J. Appl. Phys. **97**, 114327 (2005).

[12] H. Söderberg, M. Oden, T. Larsson, L. Hultman, and J. M. Molina-Aldareguia, Appl. Phys. Lett. **88**, 191902 (2006).

[13] H. Söderberg, M. Oden, A. Flink, J. Birch, P. O. A. Persson, M. Beckers, and L. Hultman, J. Mater. Res. **22**, 3255 (2007).

[14] L. Hultman, J. Bareno, A. Flink, H. Söderberg, K. Larsson, V. Petrova, M. Oden, J. E. Greene, and I. Petrov, Phys. Rev. B **75**, 155437 (2007).

[15] X. Hu, H. Zhang, J. Dai, G. Li, and M. Gu, J. Vac. Sci. Technol. A **23**, 114 (2005).

[16] Y. Dong, W. Zhao, J. Yue, and G. Li, Appl. Phys. Lett. **89**, 121916 (2006).

[17] B. Alling, E. I. Isaev, A. Flink, L. Hultman, and I. A. Abrikosov, Phys. Rev. B **78**, 132103 (2008).

[18] R. F. Zhang, A. S. Argon, and S. Veprek, Phys. Rev. B **79**, 245426 (2009).

[19] R. F. Zhang, A. S. Argon, and S. Veprek, Phys. Rev. Lett. **102**, 015503 (2009).

[20] A. Niederhofer, P. Nesladek, H.-D. Männling, K. Moto, S. Veprek, and M. Jilek, Surf. Coat. Technol. **120-121**, 173 (1999).

[21] S. Christiansen, M. Albrecht, H. P. Strunk, and S. Veprek, J. Vac. Sci. Technol. B **16**, 19 (1998).

[22] S. G. Prilliman, S. M. Clark, A. P. Alivisatos, P. Karvankova, and S. Veprek, Mater. Sci. Eng., A **437**, 379 (2006).

[23] R. F. Zhang and S. Veprek, Thin Solid Films **516**, 2264 (2008).

[24] R. F. Zhang, S. H. Sheng, and S. Veprek, Appl. Phys. Lett. **90**, 191903 (2007); **91**, 031906 (2007).

[25] R. F. Zhang, S. H. Sheng, and S. Veprek, Appl. Phys. Lett. **94**, 121903 (2009).

[26] S. Veprek and S. Reiprich, Thin Solid Films **268**, 64 (1995).

[27] P. J. Paul, Semicond. Sci. Technol. **19**, R75 (2004).

[28] S. Veprek and M. G. J. Veprek-Heijman, Surf. Coat. Technol. **201**, 6064 (2007).

[29] T. An, M. Wen, L. L. Wang, C. Q. Hu, H. W. Tian, and W. T. Zheng, J. Alloys Compd. **486**, 515 (2009).

[30] A. R. West, *Solid State Chemistry and Its Applications* (Wiley, Chicester, 1984).

[31] A. F. Wells, *Structural Inorganic Chemistry*, 5th ed. (Clarendon Press, Oxford, 1987.

[32] F. A. Cotton and G. Wilkinson, *Advanced Inorganic Chemistry*, 3rd ed. (Wiley, New York, 1972).

[33] C. S. Tian, D. Qian, D. Wu, R. H. He, Y. Z. Wu, W. X. Tang, L. F. Yin, Y. S. Shi, G. S. Dong, X. F. Jin, X. M. Jiang, F. Q. Liu, H. J. Qian, K. Sun, L. M. Wang, G. Rossi, Z. Q. Qiu, and J. Shi, Phys. Rev. Lett. **94**, 137210 (2005).

[34] X. Y. Zhang, X. L. Wu, Q. Liu, R. L. Zuo, A. W. Zhu, P. Jiang, and Q. M. Wei, Appl. Phys. Lett. **93**, 031901 (2008).

[35] K. Einarsdotter, B. Sadigh, G. Grimvall, and V. Ozolins, Phys. Rev. Lett. **79**, 2073 (1997).

[36] K. L. Chopra, M. R. Randlett, and R. H. Duff, Philos. Mag. **16**, 261 (1967).

[37] K. L. Chopra, Phys. Status Solidi **32**, 489 (1969).

[38] M. Gasgnier, L. Nevot, P. Baillif, and J. Bardolle, Phys. Status Solidi A **79**, 531 (1983).

[39] G. Kresse and J. Furthmüller, Comput. Mater. Sci. **6**, 15 (1996).

[40] J. P. Perdew and Y. Wang, Phys. Rev. B **45**, 13244 (1992).

[41] R. F. Zhang, S. Veprek, and A. S. Argon, Phys. Rev. B **77**, 172103 (2008).

[42] We caution the reader that in the plots of Figs. 1 and 4 some strains, involving decohesion are normal strains (ε), while others are shear strains (γ). The nature of the different types of loading should, however, be clear.

[43] M. G. J. Veprek-Heijman, R. G. Veprek, A. S. Argon, D. M. Parks, and S. Veprek, Surf. Coat. Technol. **203**, 3385 (2009).

[44] J. B. Levine, S. H. Tolbert, and R. B. Kaner, Adv. Funct. Mater. **19**, 3519 (2009).

[45] V. L. Solozhenko, O. O. Kurakevych, D. Andrault, Y. Le Godec, and M. Mezouar, Phys. Rev. Lett. **102**, 015506 (2009).

[46] S. Veprek, R. F. Zhang, M. G. J. Veprek-Heijman, S. H. Sheng, and A. S. Argon, Surf. Coat. Technol. **204**, 1898 (2010).

[47] S. Veprek and M. J. G. Veprek-Heijman, Surf. Coat. Technol. **202**, 5063 (2008).